European Journal of Radiology 84 (2015) 534–541

Contents lists available at ScienceDirect

European Journal of Radiology

journal homepage: www.elsevier.com/locate/ejrad

Computed tomographic features of lymphangioleiomyomatosis: Evaluation in 138 patients

Kazunori Tobino[a,b,c,*], Takeshi Johkoh[d], Kiminori Fujimoto[e], Fumikazu Sakai[f], Hiroaki Arakawa[g], Masatoshi Kurihara[c,h], Toshio Kumasaka[c,i], Kengo Koike[b], Kazuhisa Takahashi[b], Kuniaki Seyama[b,c]

[a] Department of Respiratory Medicine, Iizuka Hospital, 3-83 Yoshiomachi, Iizuka, Fukuoka 820-0018, Japan
[b] Division of Respiratory Medicine, Juntendo University Faculty of Medicine & Graduate School of Medicine, 2-1-1 Hongo, Bunkyo-Ku, Tokyo 113-8421, Japan
[c] The Study Group of Pneumothorax and Cystic Lung Diseases, 4-8-1 Seta, Setagaya-Ku, Tokyo 158-0095, Japan
[d] Department of Radiology, Kinki Central Hospital of Mutual Aid Association of Public School Teachers, Kurumazuka 3-1, Itami, Hyogo 664-0872, Japan
[e] Department of Radiology, Kurume University School of Medicine and Center for Diagnostic Imaging, Kurume University Hospital, 67 Asahi-machi, Kurume, Fukuoka 830-0011, Japan
[f] Department of Diagnostic Radiology, Saitama International Medical Center, Saitama Medical University, 1397-1 Yamane, Hidaka, Saitama 350-1298, Japan
[g] Department of Radiology, Dokkyo Medical University, 880 Kita-Kobayashi, Mibu, Tochigi 321-0293, Japan
[h] Pneumothorax Center, Nissan Tamagawa Hospital, 4-8-1 Seta, Setagaya-Ku, Tokyo 158-0095, Japan
[i] Department of Pathology, Japanese Red Cross Medical Center, 4-1-22 Hiroo, Shibuya-Ku, Tokyo 150-0012, Japan

ARTICLE INFO

Article history:
Received 22 August 2014
Received in revised form 2 December 2014
Accepted 6 December 2014

Keywords:
Lymphangioleiomyomatosis
Tuberous sclerosis
Computed tomography

ABSTRACT

Purpose: The aim was to characterize the computed tomographic (CT) findings from Japanese patients with lymphangioleiomyomatosis (LAM).
Materials and methods: CT scans of the chest, abdomen, and pelvis from 124 patients with sporadic LAM (S-LAM, mean age, 37.4 years) and 14 patients with tuberous sclerosis complex (TSC)-LAM (mean age, 35.6 years) were analyzed.
Results: Pulmonary nodules (18.8%) and hepatic angiomyolipoma (AML, 24.3%) were more common in our patients than those in previous reports. Compared with TSC-LAM, S-LAM group had a higher frequency of pulmonary nodules (28.6% vs 32.3%, $P < 0.01$) and lower frequencies of air-space consolidation (21.4% vs 2.4%, $P < 0.01$), pneumothorax (28.6% vs 8.1%, $P = 0.02$), pulmonary hilar lymphadenopathy (14.3% vs 0.8%, $P < 0.01$), renal AML (85.7% vs 17.4%, $P < 0.01$), hepatic AML (71.4% vs 17.4%, $P < 0.01$), and retrocrural lymphadenopathy (14.3% vs 1.4%, $P = 0.04$). Axial lymphatic abnormalities (i.e., thoracic duct dilatation, lymphadenopathy, and lymphangioleiomyoma) were most common in the pelvis and tended to decrease in incidence with increased distance from the pelvis.
Conclusion: The incidence of some CT findings in Japanese patients differed from those in previous reports. Axial lymphatic abnormalities noted here suggest that the origin of LAM cells may be the pelvis.

1. Introduction

Lymphangioleiomyomatosis (LAM) is an uncommon disease in females of child-bearing age and is characterized by the proliferation of abnormal smooth muscle cells (LAM cells) in the lungs and along the axial lymphatic system of the thorax, retroperitoneum, and pelvic cavity. LAM occurs in approximately 30% of females with tuberous sclerosis complex (TSC-LAM), although LAM also occurs in females without TSC (i.e., sporadic LAM [S-LAM]) [1]. Both TSC-LAM and S-LAM are associated with mutations in the *TSC* genes. A diagnosis of LAM is usually made when warranted by clinical history and a pathognomonic appearance of pulmonary cysts on chest computed tomography (CT) or identification in a pathology report of LAM cells [2,3]. Recently, clinical and radiographic characteristics of patients with LAM were described based on the analyses of a large series of patients in National Heart, Lung, and Blood Institute (NHLBI) LAM registry [4–6]. In our country, clinicopathologic findings of 46 patients with LAM were already reported [2]; however,

* Corresponding author at: Division of Respiratory Medicine, Juntendo University Faculty of Medicine & Graduate School of Medicine, 2-1-1 Hongo, Bunkyo-Ku, Tokyo 113-8421, Japan. Tel.: +81 3 5802 1063; fax: +81 3 5802 1617.
E-mail address: tobino@juntendo.ac.jp (K. Tobino).

http://dx.doi.org/10.1016/j.ejrad.2014.12.008
0720-048X/

no comparable radiologic investigations have been done. Therefore, we retrospectively examined the CT images from a large series of Japanese patients with LAM to clarify the spectrum and prevalence of radiologic findings in our country.

2. Materials and methods

2.1. Patients

This retrospective study was approved by the ethics committee of our institution (JIRB21-134). We evaluated 138 females, including 124 patients with S-LAM (age range, 21–61 years; mean, 37.4 years) and 14 patients with TSC-LAM (age range, 25–50 years; mean, 35.6 years) who had undergone at least one of the following examinations at our hospital between May 1990 and November 2009: chest CT scans (138 patients; age range, 21–61 years; mean, 37.3 years), abdominal CT scans (72 patients; age range, 22–61 years; mean, 36.9 years), and pelvic CT scans (69 patients; age range, 22–61 years; mean, 37.0 years). All patients were studied when there was no evidence infection and large pneumothorax (the presence of a visible rim of ≥2 cm between the lung margin and the chest wall). Thirty-three of 138 patients had smoking history (mean, 7.6 pack-year). Each diagnosis was established based on biopsy findings of the lungs, lymphangioleiomyoma (LALM), lymph nodes (LNs), and uterus, respectively, in 92, 18, 3, and 1 patients. One patient was diagnosed based on a cytological study of the pleural fluid. Twenty-three patients did not undergo tissue biopsies, but had characteristic clinical pictures (recurrent pneumothorax and/or chylous pleural effusion) and CT findings (diffusely scattered thin-walled pulmonary cysts). Fourteen patients with TSC were diagnosed based on established clinical criteria [7].

2.2. CT technique

All chest CT scans were obtained at the end of inspiration by the patient in a supine position. The scanning protocol consisted of reconstruction of 1–5-mm collimation sections with a high spatial frequency algorithm at 1- or 2-cm intervals. Contrast material-enhanced abdominal and pelvic CT scans were performed in 62 and 60 patients, respectively, 100 ml of iohexol [Omnipaque 300] (Daiichi-Sankyo, Tokyo, Japan) or of iopamidol [Iopamiron 300] (Bayer Schering Pharma, Osaka, Japan). The remaining patients did not receive intravenous contrast material due to a history of either allergic reactions or poor renal function.

2.3. CT image analysis

Four radiologists, each with over 15 years of experience in chest, abdominal, and pelvic CT imaging, worked independently and had knowledge of the diagnosis (LAM only). These observers, all of whom were blinded to any other clinical information about the patients, were divided into two groups and reviewed the images in random order. Disagreements regarding the CT findings were resolved by consensus between the two groups. The CT scans were obtained on a variety of scanners. Images were evaluated on the film images or a monitor: (chest, 30 patients on film images and 108 patients on a monitor; abdomen, 27 patients on film images and 45 patients on a monitor; and pelvis, 25 patients on film images and 44 patients on a monitor) at window settings appropriate for viewing the lung (window level from −500 to −800 HU; window width from 1000 to 2000 HU), the mediastinum (window level from 15 to 40 HU; window width from 300 to 400 HU), and the abdomen and pelvis (window level from 15 to 40 HU; window width from 300 to 400 HU).

2.4. Chest CT image interpretation

Pulmonary cysts, noncalcified pulmonary nodules, ground-glass opacity, air-space consolidation, thickening of the bronchovascular bundles, interlobular septal thickening, thoracic duct dilatation, pneumothorax, pleural effusion, and lymphadenopathy (of the pulmonary hilum, mediastinum, supraclavicular, and/or axillary regions) were evaluated (see online supplementary materials for further details).

2.5. Abdominal and pelvic CT image interpretation

The abdominal and pelvic CT findings included hepatic and renal masses, LALM, lymphadenopathy (of the retrocrural space, upper abdomen, pelvis, and inguen), and ascites. Hepatic and renal masses were considered to represent angiomyolipomas (AMLs) if they contained fat. More information is provided in the online supplementary material.

2.6. Lymphatic lesions

Solitary masses found in LAM patients were considered to be possible LALMs or lesions of lymphadenopathy. Therefore, we defined "lymphatic lesions" as those involving thoracic duct dilatation, lymphadenopathy, LALM, and/or solitary masses and evaluated the frequency of such lesions in each part of the body.

2.7. Statistical analysis

The interobserver variation of the extent of pulmonary cysts was evaluated using Spearman's rank correlation coefficient. The interobserver variation of the extent and size of various abnormalities was evaluated using a linear regression analysis and Bland–Altman plots [8]. The interobserver variations among findings and the predominant distribution were analyzed using the k-statistic. Interobserver agreement was then classified as poor (0.00–0.20), fair (0.21–0.40), moderate (0.41–0.60), good (0.61–0.80), or excellent (0.81–1.00). The frequencies of various findings were compared using the Chi-square test with appropriate Fisher exact test, and the extent of pulmonary cysts was compared between the S-LAM and TSC-LAM groups using the unpaired t-test. All statistical analyses were performed using the SPSS software program (version 16.0, SPSS Inc., Chicago, IL, USA). The data are expressed as the mean ± standard deviation (SD). A P-value of less than 0.05 was considered to indicate a significant difference.

3. Results

3.1. Observer agreement

Regarding the chest CT findings, there was moderate to excellent agreement with respect to the extent and size of the pulmonary cysts (Spearman rank correlation coefficient, $r = 0.607–0.942$; $P < 0.001$) and fair to excellent agreement for the extent and size of abnormal lesions (linear correlation coefficient, $r = 0.352–0.942$; $P < 0.001$). Agreement was fair to excellent for the presence of abnormal findings and the characteristics of distribution ($k = 0.228–1.00$); an exception was the presence of pulmonary nodules ($k = 0.200$). Regarding abdominal and pelvic CT findings, the existence of abnormal findings generated good to excellent agreement ($k = 0.655–1.00$) and excellent agreement for the size of abnormal lesions (linear correlation coefficient, $r = 0.947–0.966$, $P < 0.001$), with the exception of the size of intrapelvic solitary masses ($r = 0.215$, $P = 0.580$) (see online supplementary materials for further details). Bland–Altman plots of the two groups' measurements of the extent of pulmonary cysts are shown in Fig. 1.

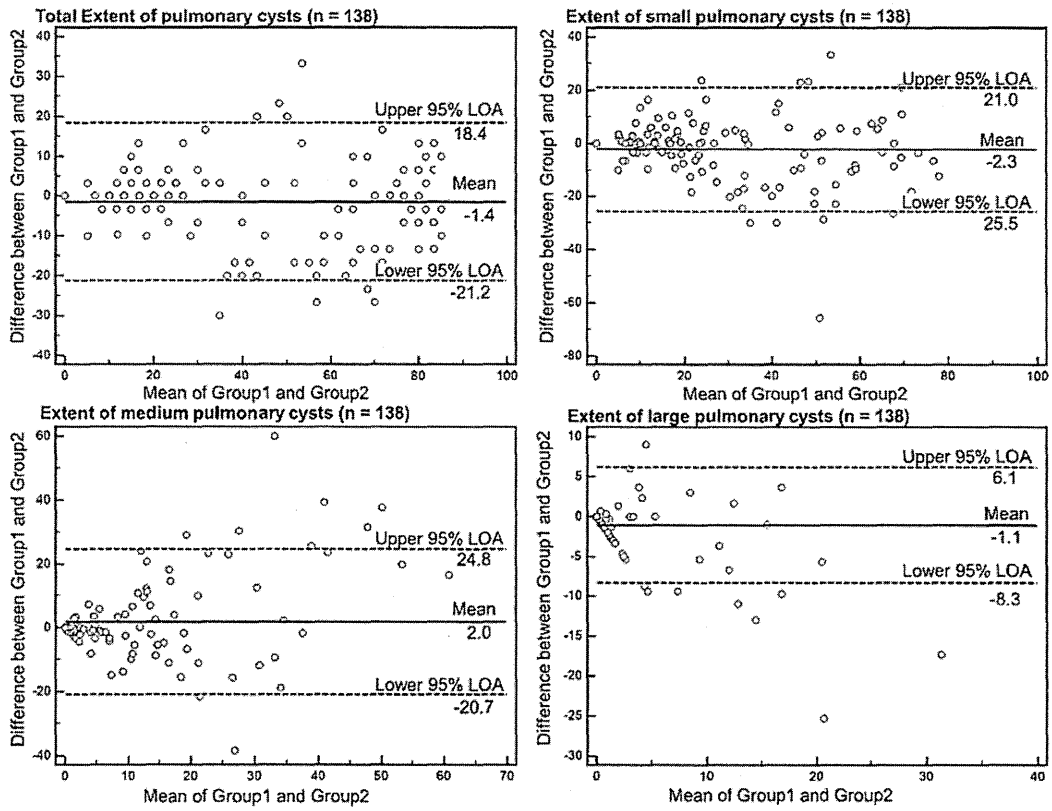

Fig. 1. Bland–Altman plots of measurements averaged across the two groups, according to lesion extent and size. Solid center line represents the mean of differences. The top dashed line shows the upper 95% limit of agreement (LOA), and the bottom dashed line shows the lower 95% LOA (±1.96 times the standard deviation).

The mean bias between the two groups was close to zero in each size category and also in total.

3.2. Chest CT findings

In our study, all but one patient had well-circumscribed, thin-walled pulmonary cysts. The total extent of pulmonary cysts on CT scans was 38.9 ± 27.9% (mean ± SD) (Table 1). Most pulmonary cysts were small (<10 mm) and distributed diffusely throughout the lungs. Most of our patients had randomly distributed pulmonary cysts.

The chest CT findings other than pulmonary cysts are also shown in Table 1. Fifty patients (36.2%) had noncalcified pulmonary nodules; of these, 26 (18.8%) had multiple (three or more) noncalcified pulmonary nodules. Ground-glass attenuation and air-space consolidation were found in seven (5.1%) and six (4.3%) patients, respectively. Thickening of the bronchovascular bundles and interlobular septal tissues were also relatively frequent (18.1% and 9.4%, respectively). Lymphadenopathy was more common in the mediastinum (8.7%) than in other regions of the thorax.

A diffusely thickened mediastinum with water attenuation was found in two patients (Fig. 2). Both patients also had pleural effusions and ground-glass attenuation.

3.3. Abdominal and pelvic CT findings

Of the 72 patients who underwent an abdominal CT, 17 (23.6%) had fat-containing masses, and three (4.2%) had uniformly enhanced masses in the kidneys (Table 2). These findings were thought to be indicative of AML; therefore, 20 (27.8%) patients may have had renal AML. Renal cysts were found in 5.6% of the present patients. Regarding the liver, 15 (20.1%) patients had fat-containing masses, and 3 (4.2%) patients had uniformly enhanced masses (Table 2). Therefore, the 18 (25.0%) patients considered to have liver AML. Liver cysts and hemangiomas were found in 13.9% and 1.4% of our patients, respectively. Lymphadenopathy was more common in the pelvis (11.6%) and abdomen (11.1%) than in other regions (Table 3). LALM afflicted 26 of 69 patients (37.7%) who underwent abdominopelvic CT, with LALM extending from the abdomen to the pelvis exhibiting the highest frequency (13.0%) (Table 3). Solitary masses were found in 14 of 69 patients (20.1%) who underwent abdominopelvic CT (Table 3). This finding was most frequently observed in the pelvis (11.8%). Nine of 72 patients (12.5%) had ascites ($k = 0.834$, $P < 0.001$).

3.4. Lymphatic lesions

The frequencies of lymphatic lesions in various areas of the body are shown in Fig. 3. Lymphatic lesions were most frequent in the pelvis (43.5%), and their numbers decreased as the distance from the pelvis increased.

3.5. Comparison of CT findings between the S-LAM and TSC-LAM groups

Statistically significant differences distinguished the S-LAM from the TSC-LAM groups. Tables 1–3 display those values for pulmonary nodules, air-space consolidation, pneumothorax formation, lymphadenopathy in the pulmonary hilum, renal AML, hepatic AML, and lymphadenopathy in the retrocrural space.

Table 1
Chest CT findings.

Findings	Total (n = 138)	S-LAM (n = 124)	TSC-LAM (n = 14)	P-value
Pulmonary cysts				
Extent (%)				
Total extent	38.9 ± 27.9	38.5 ± 28.4	43.7 ± 23.8	0.51
Small cysts	27.8 ± 20.5	27.0 ± 20.4	36.1 ± 21.0	0.12
Medium cysts	9.2 ± 13.0	9.5 ± 13.5	6.3 ± 7.0	0.38
Large cysts	2.0 ± 4.9	2.1 ± 5.1	1.4 ± 2.3	0.60
Distribution (no. of patients)				
Axial direction				
Upper predominant	8(5.8)	7(5.6)	0	0.48
Lower predominant	12(8.6)	12(9.7)	0	
Random/Diffuse	117(84.2)	104(83.9)	14(100)	
No cyst	1(0.7)	1(0.8)	0	
Horizontal direction				
Central predominant	0	0	0	0.87
Peripheral predominant	0	0	0	
Ventral predominant	3(2.2)	3(2.4)	0	
Dorsal predominant	0	0	0	
Random/diffuse	134(96.4)	120(96.8)	14(100)	
No cyst	1(0.7)	1(0.8)	0	
Pulmonary nodule	52(37.7)	42(33.9)	10(71.4)	<0.01
Nodules of <10	45(32.6)	40(32.3)	5(35.7)	<0.01
Nodules of ≥10	7(5.1)	2(1.6)	5(35.7)	
Size in patients with nodules (mm)	3.8 ± 2.8 (1.0–16.5)	3.4 ± 2.8 (1.0–16.5)	5.3 ± 2.7 (1.5–10)	0.15
Ground-glass attenuation	7(5.1)	7(5.6)	0	0.36
Extent in patients with ground-glass attenuation (%)	14.3 ± 14.2	14.3 ± 14.2	–	N/A
Air-space consolidation	6(4.3)	3(2.4)	3(21.4)	<0.01
Extent in patients with air-space consolidation (%)	4.4 ± 2.5	5.0 ± 2.5	3.9 ± 2.5	0.64
Thickening of bronchovascular bundles	25(18.1)	20(16.1)	5(35.7)	0.07
Interlobular septal thickening	13(9.4)	13(10.5)	0	0.20
Thoracic duct dilatation	5(3.6)	4(3.2)	1(7.1)	0.46
Pneumothorax	14(10.1)	10(8.1)	4(28.6)	0.02
Right side	5(3.6)	3(2.4)	2(14.3)	
Left side	8(5.8)	7(5.6)	1(7.1)	<0.01
Both sides	1(0.7)	0	1(7.1)	
Pleural effusion	15(10.8)	14(11.3)	1(7.1)	0.64
Right side	6(4.3)	5(4.0)	1(7.1)	
Left side	8(5.8)	9(7.3)	0	0.72
Both sides	1(0.7)	0	0	
Thoracic lymphadenopathy	14(10.1)	12(9.7)	2(14.3)	0.59
Mediastinum	10(7.2)	9(7.3)	1(7.1)	0.99
Pulmonary hilum	3(2.2)	1(0.8)	2(14.3)	<0.01
Supraclavicular region	1(0.7)	1(0.8)	0	0.74
Axilla	1(0.7)	1(0.8)	0	0.74

N/A: not available. Data in parenthesis are percentages.

4. Discussion

Our present study is the first to document the results from a large serial study of Japanese patients with LAM. Recently, a group at the American National Institutes of Health (NIH) reported the outcomes for similar analyses of patients with LAM [5,6]. The pathognomonic finding in chest CTs of patients with LAM is thin-walled pulmonary cysts in a random distribution. In our patients, TSC-LAM groups had a higher extent of pulmonary cysts than in some previous reports. The cause of this discrepancy may have been due to the small number of TSC-LAM patients in our study. Nevertheless, in our series, the frequency of pulmonary nodules (18.8% in total, 13.7% in S-LAM, and 64.3% in TSC-LAM) was higher than in the NIH group's study (3.4% in total, 1% in S-LAM, and 12% in TSC-LAM). The racial differences may be one cause of the difference between the two studies, because this disparity in results was confirmed when we used their definition ("multiple [three or more] noncalcified pulmonary nodules") [6].

Ground-glass attenuation and consolidation are thought to represent hemorrhage and/or edema [9]. Moreover, such findings may also indicate lymphatic edema, because six of our patients with these conditions also manifested interlobular septal thickening and/or thickening of the bronchovascular bundles, which could be an expression of interstitial lymphatic edema caused by obstruction of the lymphatic vessels [10,11].

In our series, the frequency of mediastinal lymphadenopathy was 8.7%, with no differences observed between the S-LAM and TSC-LAM groups. However, pulmonary hilar lymphadenopathy was more common in TSC-LAM than in S-LAM group [2,12]. The frequencies of thoracic duct dilatation and pleural effusion found in our patients were similar to those reported in the previous report [6]. Two of our patients exhibited diffusely thickened mediastina with decreased density. The cause may have been an increase of lymphatic fluid accumulated in the mediastinum, because pleural effusions and ground-glass attenuation present in both patients could indicate lymphatic abnormalities.

Renal AML is the most common tumor associated with LAM, and the reported frequency of renal AML is up to 90% among patients with TSC and up to 50% for patients with S-LAM [5,6,13–15]. Our S-LAM patients had a lower frequency of renal AML than in that of previous reports (27.8% in total, 17.4% in S-LAM and 85.7% in TSC-LAM). The racial difference may account for this divergence.

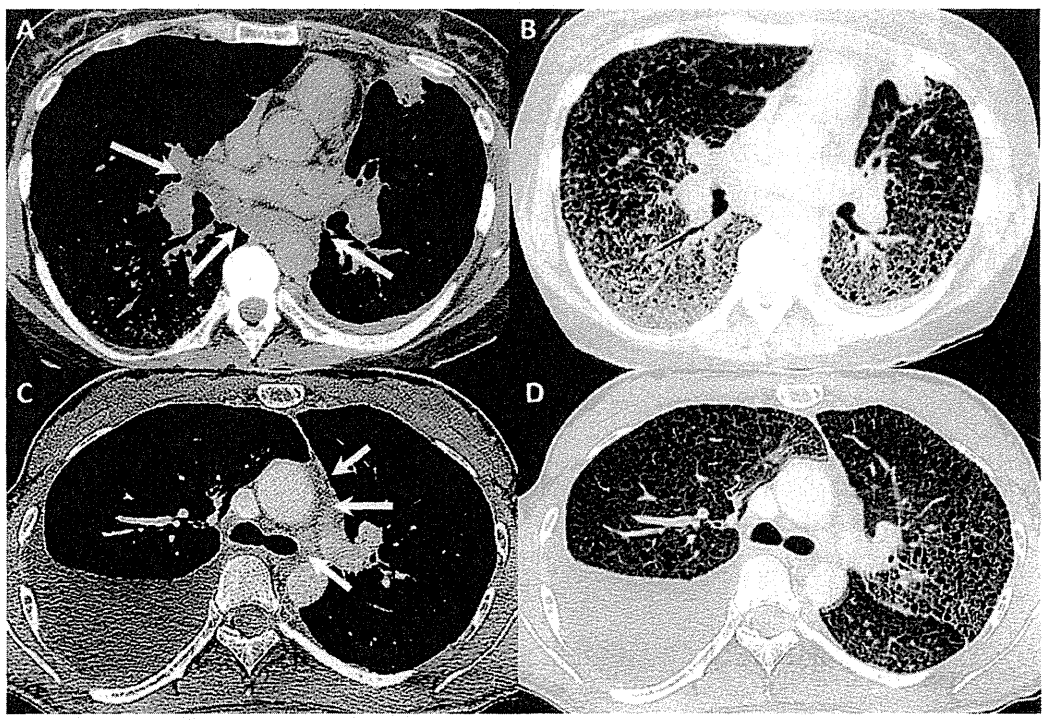

Fig. 2. CT images of a thickened mediastinum with decreased density. (A, B) CT images of a 41-year-old female with S-LAM, and (C, D) CT images of a 30-year-old female with S-LAM. The CT images of both patients show thickened mediastina with decreased density (arrows). Note the coexistence of ground-glass attenuation and pleural effusion.

Hepatic AML is a rare, benign fatty tumor. The NIH group reported the frequency of hepatic AML in LAM patients to be 8.7%, which is lower than our findings (19.4%). In our series, hepatic AML was more common in the TSC-LAM group than in the S-LAM group (57.1% vs. 15.4%, respectively), and this result also differs from that reported by the NIH (33% vs. 2%), possibly owing to racial factors. Others found hepatic AML only in association with renal AML [16]. However, both of our two patients with TSC-LAM as well as hepatic AML also had renal AML. Still, among the S-LAM patients, only four of 15 patients with hepatic AML also had renal AML. Therefore, no association was apparent between the occurrence of hepatic AML and renal AML in patients with S-LAM.

Renal cysts are acquired lesions that are thought to evolve from diverticula in the distal convoluted and collecting tubules [17]. The progression of diverticula into cysts seems to occur primarily as an age-related process in association with weakening of the tubular basement membrane [18]. As documented, the prevalence of renal and liver cysts in Japanese females 35–40 years of age

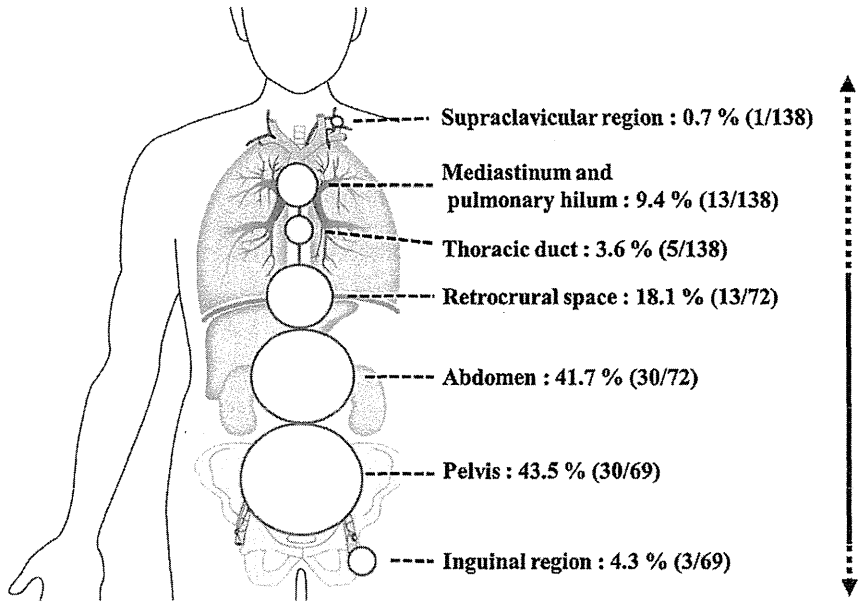

Fig. 3. Frequency of lymphatic lesions. Lymphatic lesions were most frequently observed in the pelvis, with the incidence decreasing as the distance from the pelvis increased.

Table 2
Kidney and liver findings.

Findings	Number of patients			
	Total (n = 72)	S-LAM (n = 65)	TSC-LAM (n = 7)	P-value
Kidney				
AML	20(27.8)	14(21.5)	6(85.7)	<0.01
Fat containing mass	16(24.6)	10(15.4)	6(85.7)	<0.01
Right side	5(6.9)	4(6.2)	1(14.3)	
Left side	3(4.2)	1(1.5)	2(28.6)	<0.01
Both sides	8(12.3)	5(7.7)	3(42.9)	
Fat containing mass of <10	10(15.4)	8(12.3)	3(42.9)	<0.01
Fat containing mass of ≥10	5(6.9)	2(3.1)	3(42.9)	
Size of mass in patients with this finding (mm)	41.8 ± 37.1	51.8 ± 43.8	25.2 ± 11.9	0.17
Uniformly enhanced mass	3(4.2)	2(3.1)	1(14.3)	0.16
Right side	1(1.4)	0	1(14.3)	
Left side	2(2.8)	2(3.1)	0	0.02
Both sides	0	0	0	
Uniformly enhanced mass of <10	3(4.2)	2(3.1)	1(14.3)	0.37
Uniformly enhanced mass of ≥10	0	0	0	
Size of mass in patients with this finding (mm)	15.8 ± 9.5	21.3 ± 1.8	5.0	N/A
Renal artery embolization or renal extraction	5(6.9)	4(6.2)	1(14.3)	0.42
Right side	1(1.4)	0	1(14.3)	
Left side	4(5.6)	4(6.2)	0	0.02
Both sides	0	0	0	
Cyst	4(5.6)	3(4.6)	1(14.3)	0.29
Right side	1(1.4)	0	1(14.3)	
Left side	2(2.8)	2(3.1)	0	0.02
Both sides	1(1.4)	1(1.5)	0	
Cyst of <10	4(5.6)	3(4.6)	1(14.3)	0.57
Cyst of ≥10	0	0	0	
Size of cyst in patients with this finding (mm)	4.1 ± 0.4	4.0 ± 0.5	4.5	N/A
Liver				
AML = Fat containing mass	14(19.4)	10(15.4)	4(57.1)	0.01
Fat containing mass of <10	11(15.3)	9(13.8)	2(28.6)	<0.01
Fat containing mass of ≥10	3(4.2)	1(1.5)	2(28.6)	
Size of mass in patients with this finding (mm)	15.8 ± 19.3	10.6 ± 5.9	28.8 ± 34.5	0.11
Cyst	10(13.9)	10(15.4)	0	0.26
Cyst of <10	10(13.9)	10(15.4)	0	0.54
Cyst of ≥10	0	0	0	
Size of cyst in patients with this finding (mm)	12.8 ± 17.3	12.8 ± 17.3	–	N/A
Hemangioma	1(1.4)	1(1.5)	0	0.74
Hemangioma of <10	1(1.4)	1(1.5)	0	0.95
Hemangioma of ≥10	0	0	0	
Size of hemangioma in patients with this finding (mm)	20.0	20.0	–	N/A

N/A: not available. Data in parenthesis are percentages.

is approximately 1.5% and 2%, respectively [19]. Therefore, our results suggest the probability of a high incidence of renal and hepatic cysts in LAM patients.

Enlarged LNs in the abdomen and pelvis have been described in up to 40% of patients with S-LAM, with 14% occurring in the retrocrural space, 25% in the abdomen, and 5% in the pelvis [11]. Our results showed a relatively lower incidence of lymphadenopathy in these regions. LALM is thought to result from the proliferation of LAM cells in lymphatic vessels, causing dilatation and obstruction [20]. The CT scans of patients with LALM have included large, contiguous, lobulated masses, sometimes infiltrating the retroperitoneum. The NIH group cited a 24.8%, frequency of LALM in LAM patients, which is similar to our results. Solitary masses other than LNs were apparent only in our S-LAM patients. This type of lesion is thought to be a relatively small LALM, since most of these lesions contain areas of low attenuation on CT. However, the LNs in LAM patients can measure up to 4.0 cm in diameter; therefore, some of these lesions may be LNs. Unfortunately, the small number of our TSC-LAM patients precluded a precise statistical analysis of the difference between S-LAM and TSC-LAM.

LAM cells produce VEGF-D that induces lymphangiogenesis where the cells proliferate. Accordingly, patients with LAM frequently show such abnormalities along the axial lymphatics as thoracic duct dilatation, lymphadenopathy, and LALM as well as chyle leakage into the thorax and/or abdomen [21]. The frequencies of findings related to abnormalities of the axial lymphatics in our patients are presented in Fig. 3. Axial lymphatic abnormalities were most common in the pelvis and tended to decrease in incidence with increased distance from the pelvis. This result is consistent with the histopathological incidence of lymphatic lesions identified by Kumasaka et al. in five individuals at autopsy. In their report, the axial lymphatic system, including the retroperitoneal LNs, thoracic duct, mediastinal LNs, and left supraclavicular LNs, exhibited a high rate of positive LAM lesions (88%, 100%, 68%, and 82%, respectively) [21]. However, LNs belonging to the tributaries, such as the mesenteric, axial, and cervical LNs, exhibited no or extremely low rates of positive LAM lesions (0–14%). Taking into consideration the lymphatic stream's direction, we believe the results from both radiologic and histopathologic examinations suggest that LAM cells originate in the pelvic cavity and spread via the axial lymphatic system. This presumption is supported by two pathologic studies: (1) uterine and adnexal involvement by LAM is highly prevalent as demonstrated in 9 of 10 LAM patients examined [22], and (2) LAM lesions in pelvic and paraaortic LNs were found in three patients with uterine cancer, although none of them had TSC or LAM in other organs [23].

Our study has several limitations. First, this is a retrospective, cross-sectional study that lacks longitudinal data and also detailed clinical information (i.e., clinical manifestation and pulmonary function). Second, there is a selection bias because our institution

Table 3
Findings of lymphatic lesions.

	Number of patients			
	Total	S-LAM	TSC-LAM	*P*-value
Lymphadenopathy				
Retrocrural space ($n=72$)	2(2.8)	1/65(1.5)	1/7(14.3)	0.05
Lymphadenopathy of <10	2(2.8)	1/65(1.5)	1/7(14.3)	0.15
Lymphadenopathy of ≥10	0	0	0	
Abdomen ($n=72$)	8(11.1)	6/65(9.2)	2/7(28.6)	0.12
Lymphadenopathy of <10	3(4.2)	2/65(3.1)	1/7(14.3)	0.25
Lymphadenopathy of ≥10	5(6.9)	4/65(6.2)	1/7(14.3)	
Pelvis ($n=69$)	8(11.6)	6/62(9.7)	2/7(28.6)	0.14
Lymphadenopathy of <10	2(2.9)	1/62(1.6)	1/7(14.3)	0.13
Lymphadenopathy of ≥10	6(8.7)	5/62(8.1)	1/7(14.3)	
Inguinal region ($n=69$)	3(4.3)	3/62(4.8)	0	0.40
Lymphadenopathy of <10	1(1.4)	1/62(1.6)	0	0.84
Lymphadenopathy of ≥10	2(2.9)	2/62(3.2)	0	
Lymphangioleiomyoma				
Retrocrural space ($n=72$)	10(13.9)	8/65(12.3)	2/7(28.6)	0.24
Abdomen ($n=72$)	23(31.9)	21/65(32.3)	2/7(28.6)	0.84
Pelvis ($n=69$)	17(24.6)	15/62(23.1)	2/7(28.6)	0.75
Extent of lymphangioleiomyoma ($n=69$)				
Only in the retrocrural space	1(1.4)	1/62(1.6)	0	0.27
Only in the abdomen	5(6.9)	5/62(8.1)	0	
Only in the pelvis	2(2.9)	1/62(1.6)	1/7(14.3)	
From retrocrural space to abdomen	3(4.2)	2/62(3.2)	1/7(14.3)	
From abdomen to pelvis	9(13.0)	9/62(14.5)	0	
From retrocrural space to pelvis	6(8.7)	5/62(8.1)	1/7(14.3)	
Solitary masses				
Retrocrural space ($n=72$)	2(2.8)	2/65(3.1)	0	0.64
Solitary mass of <10	2(2.8)	2/65(3.1)	0	0.90
Solitary mass of ≥10	0	0	0	
Size of mass in patients with this finding (mm)	22.0 ± 12.0	22.0 ± 12.0	–	N/A
Abdomen ($n=72$)	1(1.4)	1/65(1.5)	0	0.74
Solitary mass of <10	1(1.4)	1/65(1.5)	0	0.95
Solitary mass of ≥10	0	0	0	
Size of mass in patients with this finding (mm)	11.5	11.5	–	N/A
Pelvis ($n=69$)	9(13.0)	7/62(11.3)	2/7(28.6)	0.20
Solitary mass of <10	7(10.1)	6/62(9.7)	1/7(14.3)	0.15
Solitary mass of ≥10	2(2.9)	1/62(1.6)	1/7(14.3)	
Size of mass in patients with this finding (mm)	29.6 ± 7.4	27.7 ± 7.4	36.3 ± 1.8	0.17
Inguinal region ($n=69$)	0	0	0	N/A

N/A: not available. Data in parenthesis are percentages.

is a referral center, and the number of TSC-LAM patients included was relatively small. Moreover, because our study was a retrospective study about the patients with LAM who were referred to the respiratory department of our institution, relatively lower percentage of patients underwent abdominal and pelvic CT. However, to our knowledge, the number of patients included to our study ranks second to that in the report of Avila et al. [6]. Our result is not based on many patients with severe disease or comorbidities, because all patients were studied when there was no evidence of large pneumothorax and infection. Third, regarding evaluation of the size of intrapelvic solitary masses, the correlation between the two reader groups was not statistically significant ($r=0.215$, $P=0.580$), because so few patients had this condition. Fourth, this study is a multicenter investigation and the CT scans were obtained with a variety of scanners. However, there was little difference in CT image quality because the scanning protocols were almost uniform. Finally, not all findings exhibited pathologic correlations.

In conclusion, this study is the first to delineate in detail CT findings in a large series of Japanese patients with LAM. Notably, the incidence of some CT findings in our study differs from those in previous reports, possibly attributable to racial variations. An examination of lymphatic lesions suggests that LAM cells may originate in the pelvis then spread via the axial lymphatic system. Because medical diagnosis and treatment are subject to the uniqueness of human populations, global comparisons significantly enhance our ability to alleviate disease.

Conflict of interest

The authors declare there are no conflicts of interest.

Acknowledgements

We thank Dr. Yoshihito Hoshika of the Department of Respiratory Medicine, Juntendo University Hospital, and the medical technologists including Mr. Toyoaki Takahashi, Mr. Hideaki Sudo, and Mr. Kazuhiko Doryo of the Department of Radiology, Juntendo University Hospital for their assistance in obtaining the CT data. This study was supported in part by a grant to the Respiratory Failure Research Group from the Ministry of Health, Labour and Welfare, Japan, a High Technology Research Center Grant from the Ministry of Education, Culture, Sports, Science and Technology, Japan, and the Institute for Environmental and Gender-Specific Medicine, Juntendo University, Graduate School of Medicine. We thank Ms. Phyllis Minick for her excellent proofreading of our English writing.

Appendix A. Supplementary data

Supplementary data associated with this article can be found, in the online version, at http://dx.doi.org/10.1016/j.ejrad.2014.12.008.

References

[1] McCormack FX. Lymphangioleiomyomatosis: a clinical update. Chest 2008;133:507–16.

[2] Kitaichi M, Nishimura K, Itoh H, Izumi T. Pulmonary lymphangioleiomyomatosis: a report of 46 patients including a clinicopathologic study of prognostic factors. Am J Respir Crit Care Med 1995;151:527–33.

[3] Johnson SR, Cordier JF, Lazor R, Cottin V, Costabel U, Harari S, et al. Review Panel of the ERS LAM Task Force European Respiratory Society guidelines for the diagnosis and management of lymphangioleiomyomatosis. Eur Respir J 2010;35:14–26.

[4] Ryu JH, Moss J, Beck GJ, Lee JC, Brown KK, Chapman JT, et al. NHLBI LAM Registry Group. The NHLBI lymphangioleiomyomatosis registry: characteristics of 230 patients at enrollment. Am J Respir Crit Care Med 2006;173:105–11.

[5] Avila NA, Kelly JA, Chu SC, Dwyer AJ, Moss J. Lymphangioleiomyomatosis: abdominopelvic CT and US findings. Radiology 2000;216:147–53.

[6] Avila NA, Dwyer AJ, Rabel A, Moss J. Sporadic lymphangioleiomyomatosis and tuberous sclerosis complex with lymphangioleiomyomatosis: comparison of CT features. Radiology 2007;242:277–85.

[7] Roach ES, Gomez MR, Northrup H. Tuberous sclerosis complex consensus conference: revised clinical diagnostic criteria. J Child Neurol 1998;13:624–8.

[8] Bland JM, Altman DG. Statistical methods for assessing agreement between two methods of clinical measurement. Lancet 1986;1:307–10.

[9] Pallisa E, Sanz P, Roman A, Majó J, Andreu J, Cáceres J. Lymphangioleiomyomatosis: pulmonary and abdominal findings with pathologic correlation. Radiographics 2002;22:S185–98.

[10] Lenoir S, Grenier P, Brauner MW, Frija J, Remy-Jardin M, Revel D, et al. Pulmonary lymphangiomyomatosis and tuberous sclerosis: comparison of radiographic and thin-section CT findings. Radiology 1990;175:329–34.

[11] Sullivan EJ. Lymphangioleiomyomatosis: a review. Chest 1998;114:1689–703.

[12] Kirchner J, Stein A, Viel K, Dietrich CF, Thalhammer A, Schneider M, et al. Pulmonary lymphangioleiomyomatosis: high-resolution CT findings. Eur Radiol 1999;9:49–54.

[13] Chao CH, Lin CY, Chan SC, Chen KS. Concurrent hepatic and ruptured renal angiomyolipoma in tuberous sclerosis complex. Chang Gung Med J 2004;27:696–700.

[14] Casper KA, Donnelly LF, Chen B, Bissler JJ. Tuberous sclerosis complex: renal imaging findings. Radiology 2002;225:451–6.

[15] Neumann HP, Schwarzkopf G, Henske EP. Renal angiomyolipomas, cysts, and cancer in tuberous sclerosis complex. Semin Pediatr Neurol 1998;5:269–75.

[16] Jóźwiak S, Pedich M, Rajszys P, Michalowicz R. Incidence of hepatic hamartomas in tuberous sclerosis. Arch Dis Child 1992;67:1363–5.

[17] Pedersen JF, Emamian SA, Nielsen MB. Simple renal cyst: relations to age and arterial blood pressure. Br J Radiol 1993;66:581–4.

[18] Baert L, Steg A. Is the diverticulum of the distal and collecting tubules a preliminary stage of the simple cyst in the adult? J Urol 1977;118:707–10.

[19] Mitsumine T, Kayashima E, Ohkuchi S, Nananishi T. Statistics of benign findings of liver, gallbladder, and kidney detected at abdominal ultrasonography. Health Eval Promot 2009;36:361–4.

[20] Carrington CB, Cugell DW, Gaensler EA, Marks A, Redding RA, Schaaf JT, et al. Lymphangioleiomyomatosis. Physiologic–pathologic–radiologic correlations. Am Rev Respir Dis 1977;116:977–95.

[21] Kumasaka T, Seyama K, Mitani K, Souma S, Kashiwagi S, Hebisawa A, et al. Lymphangiogenesis-mediated shedding of LAM cell clusters as a mechanism for dissemination in lymphangioleiomyomatosis. Am J Surg Pathol 2005;29:1356–66.

[22] Hayashi T, Kumasaka T, Mitani K, Terao Y, Watanabe M, Oide T, et al. Prevalence of uterine and adnexal involvement in pulmonary lymphangioleiomyomatosis: a clinicopathologic study of 10 patients. Am J Surg Pathol 2011;35:1776–85.

[23] Iwasa Y, Tachibana M, Ito H, Iwami S, Yagi H, Yamada S, et al. Extrapulmonary lymphangioleiomyomatosis in pelvic and paraaortic lymph nodes associated with uterine cancer: a report of 3 cases. Int J Gynecol Pathol 2011;30:470–5.

RESPIRATORY INVESTIGATION 52 (2014) 274–276

Contents lists available at ScienceDirect

Respiratory Investigation

journal homepage: www.elsevier.com/locate/resinv

Letter to the Editor

What's the role of sirolimus on the treatment of lymphangioleiomyomatosis (LAM)?: Merely tuning up of LAM-associated dysfunctional lymphatic vessels rather than cytoreduction?

To the Editor,

In a recent study, we reported the efficacy and safety of low sirolimus doses for the treatment of lymphangioleiomyomatosis (LAM) [1]. One of the representative LAM patients, JUL97 had complicated Aspergillus infection in a large destructive airspace caused by LAM in her right upper lobe while she was being administered sirolimus and had undergone right upper lobectomy. The sirolimus trough level in the blood was 1.2 ng/mL. Montero et al. had previously reported the radical reduction in the number of LAM cells in explanted lungs from six patients treated with sirolimus before lung transplantation [2]. On the contrary, the pathologic findings of our patient supported the notion that sirolimus exerts cytostatic rather than cytoreductive effects on LAM cells (Fig. 1).

LAM is associated with the dysregulated mammalian target of rapamycin complex 1 (mTORC1) signaling, a key regulatory pathway of protein synthesis, cell growth, and energy metabolism due to TSC gene mutation. This pathobiologic mechanism is the basis for molecular targeting of mTORC1 by sirolimus in LAM patients. The Multicenter International Lymphangioleiomyomatosis Efficacy and Safety of Sirolimus (MILES) trial successfully demonstrated that sirolimus stabilized pulmonary function in LAM patients; however, cessation of sirolimus therapy caused recurrence of progressive pulmonary function decline [3]. This supports the hypothesis that sirolimus is cytostatic.

Undoubtedly, sirolimus brought a great clinical impact on our patient since (1) she got rid of pulmonary lymphedema, a copious amount of chylohemosputum, and supplemental oxygen, (2) pulmonary function greatly improved, so that the right upper lobectomy was enabled to perform, and (3) she has been inactive for lung transplantation even after right upper lobectomy as far as she continues to take sirolimus [1]. We tried to determine the reason for the significant clinical impact observed in spite of the remaining large LAM cell number. Sirolimus is reported to be a potent inhibitor of lymphangiogenesis even at doses as low as 1 ng/mL [4] as well as to down-regulate the expression of vascular endothelial growth factor receptor-3 (VEGFR-3) by lymphatic endothelial cells [5]. In addition, sirolimus also decreased the serum levels of VEGF-D, a potent lymphangiogenic growth factor produced by LAM cells [3]. Our patient did have a lowered serum VEGF-D level while on sirolimus [1]. Resolution of pulmonary lymphedema as well as chylous pleural effusion and/or ascites with sirolimus therapy has also been reported by others [6]. Based on these findings, we hypothesize that the patient in this case benefited greatly from the low sirolimus doses owing to the fact that sirolimus inhibits LAM-associated lymphangiogenesis and "tunes up" their dysfunctional and leaky properties instead of reducing the number of LAM cells.

Conflict of interest

Kuniaki Seyama was paid travel expenses by the LAM foundation to attend the LAMposium 2013 in Cincinnati. The other authors have no conflicts of interest.

Acknowledgments

We would like to thank Ms. Phyllis Minick for her assistance in reviewing the language of this paper.

http://dx.doi.org/10.1016/j.resinv.2014.02.004

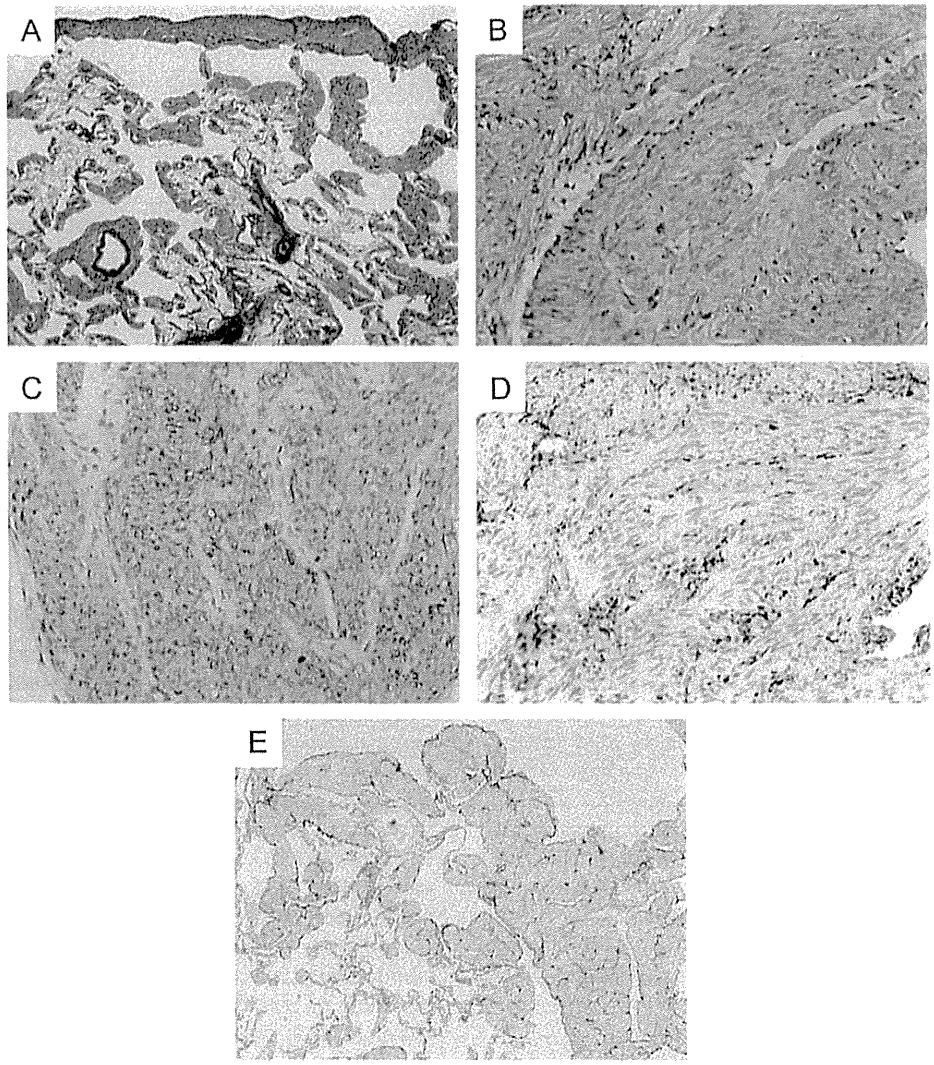

Fig. 1 – Histopathlogical findings of the resected right upper lobe post sirolimus treatment. The excised lung contained a large number of LAM cells in the parenchyma and visceral pleura ((A) Masson–Trichrome stain). A minimal amount of collagen tissue was noted within the LAM nodules. A high-magnification photomicrograph demonstrated bundles of spindle-shaped cells with cigar-shaped nuclei and eosinophilic cytoplasm proliferated in a nodular and whirling pattern ((B) hematoxylin–eosin stain). The proliferating cells were immunopositive for α-smooth muscle actin (C) as well as for HMB45 (D); therefore, they were confirmed to be LAM cells. However, slit-like clefts within the LAM nodule, indicative of LAM-associated lymphatic vessels, were not as noticeable as usual. This was confirmed by imunohistochemical analysis with a lymphatic endothelial cell ((E) D2-40 immunostaining) marker.

REFERENCES

[1] Ando K, Kurihara M, Kataoka H, et al. The efficacy and safety of low-dose sirolimus for treatment of lymphagnioleiomyomatosis. Respir Investig 2014 ([in press]).

[2] Montero MA, Roman A, Berastegui C. Radical reduction of smooth muscle cells in explanted lung of a LAM patient treated with sirolimus: first case report. J Heart Lung Transplant 2012;31:439–40.

[3] McCormack FX, Inoue Y, Moss J, et al. Efficacy and safety of sirolimus in lymphangioleiomyomatosis. N Engl J Med 2011;364:1595–606.

[4] Huber S, Bruns CJ, Schmid G, et al. Inhibition of the mammalian target of rapamycin impedes lymphangiogenesis. Kidney Int 2007;71:771–7.

[5] Luo Y, Liu L, Rogers D, et al. Rapamycin inhibits lymphatic endothelial cell tube formation by down-regulating vascular endothelial growth factor receptor 3 protein expression. Neoplasia 2012;14:228–37.

[6] Moua T, Olson EJ, Jean HC, et al. Resolution of chylous pulmonary congestion and respiratory failure in LAM with sirolimus therapy. Am J Respir Crit Care Med 2012;186:389–90.

Kentaro Suina M.D.*, Kazuhisa Takahashi
Division of Respiratory Medicine, Juntendo University Faculty of Medicine and Graduate School of Medicine, 2-1-1 Hongo, Bunkyo-Ku, Tokyo 113-8421, Japan
E-mail addresses: ksuina@juntendo.ac.jp (K. Suina), katakaha@juntendo.ac.jp (K. Takahashi)

Takuo Hayashi, Keiko Mitani
Department of Human Pathology, Juntendo University Faculty of Medicine and Graduate School of Medicine, 2-1-1 Hongo, Bunkyo-Ku, Tokyo 113-8421, Japan
E-mail addresses: tkhyz@juntendo.ac.jp (T. Hayashi), m-kei@juntendo.ac.jp (K. Mitani)

Kenji Suzuki
Department of Thoracic Surgery, Juntendo University Faculty of Medicine and Graduate School of Medicine, 2-1-1 Hongo, Bunkyo-Ku, Tokyo 113-8421, Japan
E-mail address: kjsuzuki@juntendo.ac.jp

Kuniaki Seyama
Division of Respiratory Medicine, Juntendo University Faculty of Medicine and Graduate School of Medicine, 2-1-1 Hongo, Bunkyo-Ku, Tokyo 113-8421, Japan
The Study Group of Pneumothorax and Cystic Lung Diseases, 4-8-1 Seta, Setagaya-Ku, Tokyo 158-0095, Japan
E-mail address: kseyama@juntendo.ac.jp

6 December 2013

22 February 2014

26 February 2014

*Corresponding author. Tel.: þ 81 3 5802 1063; fax: þ 81 3 5802 1617.

Lung (2014) 192:583–587
DOI 10.1007/s00408-014-9598-1

Thoracic Endometriosis-Related Pneumothorax Distinguished From Primary Spontaneous Pneumothorax in Females

Takahiro Haga · Hideyuki Kataoka · Hiroki Ebana · Mizuto Otsuji · Kuniaki Seyama · Koichiro Tatsumi · Masatoshi Kurihara

Received: 19 March 2014 / Accepted: 26 April 2014 / Published online: 16 May 2014

Abstract

Purpose Thoracic endometriosis-related pneumothorax (TERP) is a secondary condition specific for females, but in a clinical setting, TERP often is difficult to distinguish from primary spontaneous pneumothorax (PSP) based on a relationship between the dates of pneumothorax and menstruation. The purpose of this study was to clarify the clinical features of TERP compared with PSP.

Methods We retrospectively reviewed the clinical and histopathological files of female patients with pneumothorax who underwent video-assisted thoracoscopic surgery in the Pneumothorax Research Center during the 6-year period from January 2005 to December 2010. We analyzed the clinical differences between TERP and PSP.

Results The study included a total of 393 female patients with spontaneous pneumothorax, of whom 92 (23.4 %) were diagnosed as having TERP and 33.6 % (132/393) as having PSP. We identified four factors (right-sided pneumothorax, history of pelvic endometriosis, age ≥31 years, and no smoking history) that were statistically significant for predicting TERP and assigned 6, 5, 4, and 3 points, respectively, to establish a scoring system with a calculated score from 0 to 18. The cutoff values of a calculated score ≥12 yielded the highest positive predictive value (86 %; 95 % confidence interval (CI) 81.5–90.5 %) for TERP and negative predictive value (95.2 %; 95 % CI 92.3–98 %) for PSP.

Conclusions TERP has several distinct clinical features from PSP. Our scoring system consists of only four clinical variables that are easily obtainable and enables us to suspect TERP in female patients with pneumothorax.

Keywords Primary spontaneous pneumothorax · Thoracic endometriosis-related pneumothorax · Thoracic endometriosis · Pneumothorax

A1 T. Haga · H. Kataoka · H. Ebana · M. Otsuji · M. Kurihara (✉)
A2 Pneumothorax Research Center and Division of Thoracic
A3 Surgery, Nissan Tamagawa Hospital, 4-8-1 Seta,
A4 Setagaya-ku, Tokyo 158-0095, Japan
A5 e-mail: kuri@tf6.so-net.ne.jp

A6 T. Haga · K. Tatsumi
A7 Department of Respirology, Graduate School of Medicine, Chiba
A8 University, 1-8-1 Inohana, Chuo-ku, Chiba 260-8670, Japan

A9 T. Haga · H. Kataoka · H. Ebana · M. Otsuji · K. Seyama ·
A10 M. Kurihara
A11 The Study Group of Pneumothorax and Cystic Lung Diseases,
A12 4-8-1 Seta, Setagaya-ku, Tokyo 158-0095, Japan

A13 H. Ebana · K. Seyama
A14 Division of Respiratory Medicine, Juntendo University Faculty
A15 of Medicine and Graduate School of Medicine, 2-1-1 Hongo,
A16 Bunkyo-ku, Tokyo 113-8421, Japan

A17 H. Ebana · M. Otsuji
A18 Division of Thoracic and Cardiovascular Surgery, Tokyo
A19 Metropolitan Bokutoh Hospital, 4-23-15 Koto-bashi,
A20 Sumida-ku, Tokyo 130-8575, Japan

Introduction

Spontaneous pneumothorax is classified into primary (PSP) and secondary categories. PSP refers to a spontaneously occurring air leakage into the pleural space in patients with no clinically apparent underlying lung disease [1]. The diagnosis of PSP is confirmed histopathologically with subpleural blebs and bullae and no obvious abnormality in pulmonary parenchyma [2]. Catamenial pneumothorax is a condition limited to females and reported to account for approximately 20–30 % of women with pneumothorax [3, 4]. It is defined simply by the onset of pneumothorax

during a menstrual cycle: the pneumothorax that occurs between 24 h before and 72 h after the initiation of menses [5]. Because catamenial pneumothorax is usually caused by thoracic endometriosis [6, 7], a large part of catamenial pneumothorax is diagnosed as thoracic endometriosis-related pneumothorax (TERP) after thoracic surgery. However, catamenial pneumothorax may include female patients with PSP that happens to occur in the perimenstrual period.

TERP is defined as pneumothorax due to thoracic endometriosis, and the diagnosis of TERP requires histopathological confirmation [5]. Generally, ectopic endometrial tissues are found in the diaphragm in TERP, whereas no abnormality in pulmonary parenchyma is apparent. The mechanism of TERP has been speculated as follows: (1) air enters into the thoracic cavity from the peritoneum through a diaphragmatic defect caused by the implantation of endometrial tissues. This air in the peritoneum may be from outside the body and pass through ovarian tubes [8]. (2) Alternatively, air enters into the thoracic cavity from the airway through a defect of visceral pleura caused by the implantation of endometrial tissues [9, 10].

Until recently, TERP had been thought to develop only as catamenial pneumothorax. However, Alifano et al. [11] recently reported that 37.9 % of TERP cases developed as non-catamenial pneumothorax. Accordingly, TERP is difficult to distinguish from PSP based on the relationship between the calendar dates of pneumothorax and menstruation; theoretically, catamenial TERP, non-catamenial TERP, catamenial PSP, and non-catamenial PSP exist. Furthermore, TERP is virtually indistinguishable from PSP based on the findings of imaging tests, such as chest X-ray and computed tomography (CT), because the amount of ectopic endometrial tissue implanted within the respiratory system is too small for detection by such examinations [5]. A preferable scenario is that TERP is suspected before surgery, because the approaches for therapy as well as the recurrence rate [12, 13] are quite different between TERP and PSP.

As previously described, the clinical features of TERP are right-sided pneumothorax and a history of pelvic endometriosis [5]. In contrast, patients with PSP tend to be tall [14] and usually have a smoking history [15, 16]. However, few reports have compared directly the clinical features of TERP and PSP nor do they clarify the significance of each clinical variable. The purpose of this study was to clarify the clinical features of TERP compared with PSP.

Methods

Study Population

The clinical and histopathological files of all female patients who underwent video-assisted thoracoscopic surgery (VATS) in the Pneumothorax Research Center during the 6-year period from January 2005 to December 2010 were retrospectively reviewed. The patients who were histopathologically diagnosed as having TERP or PSP were included in this study. According to Alifano et al. [11], we made a diagnosis of TERP when the existence of endometrial stroma or the endometrial glands in the resected diaphragm and/or lung tissue was confirmed immunohistochemically by the presence of strong nuclear staining for either estrogen or progesterone receptors. The diagnosis of PSP was made when (1) pneumothorax occurred in otherwise healthy individuals with normal or essentially normal underlying lungs on CT images of the chest, and (2) blebs and/or bullae were histologically confirmed in the resected lung specimen. In patients with PSP, we were unable to collect information from medical records on the relationship between the occurrence of pneumothorax and menstrual cycle.

For patients with TERP and PSP, we compared the ages, pneumothorax side, height, body weight, smoking habits, history of pelvic endometriosis, number of pneumothorax episodes before surgery, duration of follow-up after surgery, and postoperative recurrence rate. We assigned the scores to each clinical variables found to be an independent predictor for the diagnosis of TERP, weighted according to the beta-coefficients from the multivariate logistic model [17]. We calculated a total score for each patient and analyzed the performance characteristics of the score for the diagnosis of TERP. The study was approved by the institutional review board of Nissan Tamagawa Hospital (approval number 12-012).

Statistical Analysis

The quantitative data are presented as mean ± SD. The differences between the patients with TERP and PSP were analyzed using the Chi square test for categorical variables and Student's t test for quantitative variables. A multiple logistic regression analysis was used to assess the role of several variables as predictive factors for TERP. The contribution of each potential predictive factor was denoted by an odds ratio and the associated 95 % confidence interval (CI). A receiver operating characteristic (ROC) curve was used to analyze the probability of TERP diagnosis in dependence on the calculated score. A value of $p < 0.05$ was considered to be significant. A statistical software package (JMP, version 10.0.2; SAS Institute; Cary, NC) was used for the statistical analysis.

Results

In total, 562 female patients with spontaneous pneumothorax were admitted for treatment during the 6-year study

Table 1 Characteristics of study population

	Patients with TERP ($n = 92$)	Patients with PSP ($n = 132$)	p value
Age (years) (range)	38.6 ± 5.7 (24–50)	27.7 ± 9.8 (14–67)	<0.01
Side of pneumothorax			
Right	91 (98.9 %)	56 (42.4 %)	<0.01
Left	1 (1.1 %)	76 (57.6 %)	
Height (cm)	159.0 ± 4.9	160.9 ± 5.9	<0.05
Weight (kg)	49.1 ± 5.7	47.6 ± 6.1	0.074
Smoking habit			
Current/former smoker	6 (6.5 %)	41 (31.1 %)	<0.01
Nonsmoker	86 (93.5 %)	91 (68.9 %)	
History of pelvic endometriosis	54 (58.7 %)	3 (2.3 %)	<0.01
The number of preoperative pneumothorax episodes	8.1 ± 3.2	2.8 ± 1.6	<0.01
Postoperative follow-up period (months)	36.2 ± 22.3	12.0 ± 11.8	<0.01
Number of patient with postoperative recurrence	36 (39.1 %)	23 (17.4 %)	<0.01

period. Of these, 393 patients underwent VATS for pneumothorax. Ninety-two (23.4 %) of the 393 patients were diagnosed as having TERP and 33.6 % (132/393) as having PSP. Thirty (32.6 %) of the 92 patients with TERP had catamenial pneumothorax with the remainder (62/92, 67.4 %) classified as non-catamenial.

Characteristics of the study population are summarized in Table 1. The patients with TERP showed significantly distinct features differing from those in the patients with PSP. The TERP group was older, shorter, and usually had right-sided pneumothorax plus pelvic endometriosis but little or no history of smoking. Many preoperative pneumothorax episodes were noted. One exception was a patient with TERP whose pneumothorax was left-sided. The postoperative recurrence of pneumothorax was more frequently noted in patients with TERP.

To find the predictive factors for TERP, we performed multivariable analysis (Table 2). The right-sided pneumothorax showed the greatest odds ratio among the other predictive factors, followed by history of pelvic endometriosis, age ≥31 years, no smoking history, the number of preoperative pneumothorax episodes ≥4, and height ≤159 cm in that order.

Next, we assigned a score to each predictive factor to establish discriminant analysis between TERP and PSP. We excluded two factors—height and the number of preoperative pneumothorax episodes—from the discriminant analysis, because these are likely to be greatly influenced

Table 2 Factors predicting TERP

Risk factors	Odds ratio	95 % CI	p value	Score assigned[a]
Right pneumothorax	440.3	15–12943.4	<0.01	6
History of pelvic endometriosis	115.1	10.2–1306.2	<0.01	5
Age ≥31 year	78.0	12.1–502.1	<0.01	4
No history of smoking	13.4	3–61	<0.01	3
Number of preoperative pneumothorax episodes ≥4	5.8	1.4–23.6	<0.05	NA
Height ≤159 cm	4.1	1.2–14.2	<0.05	NA

Calculated score = Right pneumothorax (score 6 or 0) + history of pelvic endometriosis (score 5 or 0) + age ≥31 years old (score 4 or 0) + no history of smoking (score 3 or 0)

NA not adopted

[a] If each risk factor does not exist, the score "0" is given in the following equation

by race and the medical treatment available for pneumothorax; additionally, these two factors interfered with generalizing the outcome. Accordingly, we adopted the four factors to which scores of 3–6 were assigned then established a system with calculated scores from 0 to 18 (Table 2). These scores were tested at different cutoff values. The cutoff values of a calculated score ≥12 yielded the highest positive predictive value (86 % with 95 % CI 81.5–90.5 %) for TERP and negative predictive value (95.2 % with 95 % CI of 92.3–98 %) for PSP (Table 3). The ROC curve reflects the accuracy of the diagnostic test: area under the curve was 0.9665 (Fig. 1).

Discussion

We found that TERP had distinct clinical features compared with those of PSP, enabling us to establish a simple scoring system to distinguish TERP from PSP. We demonstrated that this system had a satisfactorily high positive predictive value for TERP as well as a negative one for PSP. The scoring system utilizes four clinical variables identified here that are easily obtainable by history taking and physical examination: the side of pneumothorax, history of pelvic endometriosis, patient age, and smoking history. These clinical variables have been reported in the literature to be associated with TERP or PSP [5, 14–16]. Although a concrete diagnosis of TERP is required for histologic examination of the diaphragm or the lung tissue, the scoring system developed here seems to be suitable for suspecting TERP, thereby reducing the oversight of TERP in female patients with pneumothorax.

Table 3 Diagnostic significance of calculated score to differentiate between TERP and PSP

	Sensitivity	Specificity	Positive predictive value	Negative predictive value
Calculated score ≥12	0.935 (0.902–0.967)	0.894 (0.854–0.934)	0.86 (0.815–0.905)	0.952 (0.923–0.98)

Numbers in parentheses indicate 95 % confidence interval

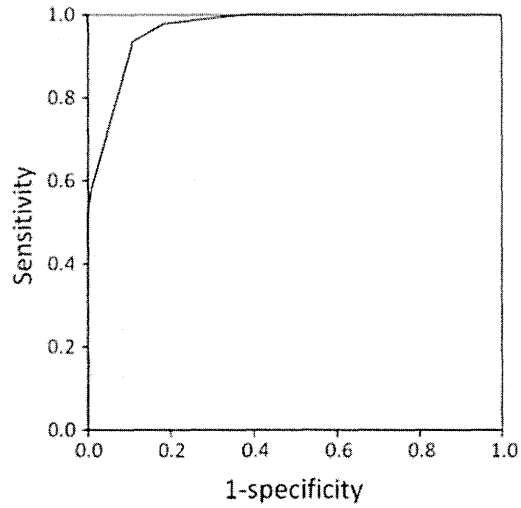

Fig. 1 ROC curve for the prediction of TERP using the calculated score. Note that the score of 12 gives 93.5 % of sensitivity and 89.4 % of specificity. The method for calculating the score appears in the footnote of Table 2

Catamenial pneumothorax has been reported to occur on the right side in almost all such cases [5], and only two case reports of left catamenial pneumothorax [9, 18] and two case reports of bilateral catamenial pneumothorax [19, 20] exist. However, those reports lacked information about the histopathological diagnosis of thoracic endometriosis. This study thus provides the first description of a left-sided TERP based on a histopathological diagnosis. PSP has no documented laterality so far [2]. Therefore, the presence of left pneumothorax in females has a high diagnostic value for PSP.

Evaluating the past history of pelvic endometriosis is valuable for diagnosing TERP in female patients with pneumothorax. In this study, 58.7 % (54/92) of the patients with TERP had a history of pelvic endometriosis. The percentage of patients with pelvic endometriosis among those with catamenial pneumothorax varies broadly and is reported to be 18–84 % [4, 21]. In the majority of patients with thoracic endometriosis, the condition is believed to have spread from pelvic endometriosis [5]. Therefore, the variations in published results are likely due to the different methods used to diagnose pelvic endometriosis. A definitive diagnosis of pelvic endometriosis requires diagnostic laparoscopy, and results from that procedure indicate that the prevalence of pelvic endometriosis among patients of reproductive age is 5–10 % [22]. In the present study, 2.3 % (3/132) of the patients with PSP had a history of pelvic endometriosis.

Previous analyses of catamenial pneumothorax calculated a mean age within the 30 s with a range in such patients from 15 to 54 years [5]. However, patients with PSP are often in their early 20 s but rarely beyond the age of 40 years [2]. The mean age of patients with TERP examined in this study was approximately 10 years older than that of patients with PSP. Therefore, it is important to consider the patient's age when diagnosing TERP in female patients with pneumothorax.

Habitual smoking has been associated with a risk of developing PSP [15, 16]; additionally, patients with PSP tended to be taller than control patients in a previous study [14]. Elsewhere, TERP did not correlate with either the patients' height or habitual smoking [5]. The results of our study are consistent with these findings.

This study has several limitations. First, our subjects were located at the Pneumothorax Research Center, which is specialized for the treatment of pneumothorax and where many patients with intractable pneumothorax are referred. Accordingly, clinical features for TERP and PSP may be biased. Second, we included only the patients with PSP whose diagnoses were confirmed histologically. Because we usually resect lung tissue only when large and/or multiple bullae are apparent during surgery, the patients with PSP in our study may represent a biased population that is not representative for PSP. Third, we could not have evaluated the significance of the onset of pneumothorax during a menstrual cycle as a factor in differentiating TERP from PSP, because no information about the relationship of pneumothorax onset and menstrual period was obtainable for the patient with PSP. Finally, because this was a retrospective cohort study, a prospective study to validate our scoring system is needed.

In conclusion, we have established a scoring system for the diagnosis of TERP that is based on the assignment of weighted values to easily include four clinical variables. This system has a highly positive predictive value for TERP as well as a negative predictive value for PSP. This logical scheme provides a useful tool for predicting TERP in the care of female patients with pneumothorax.

Acknowledgments The authors thank Ms. Phyllis Minick for her excellent proofreading of English writing.

Conflict of interest None of the authors has any conflicts of interest with regard to this study.

References

1. Noppen M, De Keukeleire T (2005) Pneumothorax. Respiration 76:121–127
2. Baumann MH, Strange C, Heffner JE et al (2001) Management of spontaneous pneumothorax: an American College of Chest Physicians Delphi consensus statement. Chest 119:590–602
3. Alifano M, Roth T, Mamilleri Broet SC, Schussler O, Magdeleinat P, Regnard JF (2003) Catamenial pneumothorax; a prospective study. Chest 124:1004–1008
4. Joseph J, Sahn SA (1996) Thoracic endometriosis syndrome: new observation from an analysis of 110 cases. Am J Med 100:164–170
5. Alifano M, Trisolini R, Cancellieri A, Regnard JF (2006) Thoracic endometriosis: current knowledge. Ann Thorac Surg 81:761–769
6. Korom S, Canyurt H, Missbach A et al (2004) Catamenial pneumothorax revisited: clinical approach and systematic review of the literature. J Thorac Cardiovasc Surg 128:502–508
7. Channabasavaiah AD, Joseph JV (2010) Thoracic endometriosis: revisiting the association between clinical presentation and thoracic pathology based on thoracoscopic findings in 110 patients. Medicine (Baltimore) 89:183–188
8. Maurer CR, Schaal JA, Mendez FL (1958) Chronic recurring spontaneous pneumothorax due to endometriosis of the diaphragm. JAMA 168:2013–2014
9. Rossi NP, Goplerud CP (1974) Recurrent catamenial pneumothorax. Arch Surg 109:173–176
10. Lillington GA, Mitchell SP, Wood GA (1972) Catamenial pneumothorax. JAMA 219:1328–1332
11. Alifano M, Jablonski C, Kadiri H et al (2007) Catamenial and noncatamenial, endometriosis-related or nonendometriosis-related pneumothorax referred for surgery. Am J Respir Crit Care Med 176:1048–1053
12. Hooper C, Maskell N (2011) British Thoracic Society national pleural procedures audit 2010. Thorax 66:636–637
13. Tschopp JM, Rami-Porta R, Noppen M, Astoul P (2006) Management of spontaneous pneumothorax: state of the art. Eur Respir J 28:637–650
14. Sadikot RT, Greene T, Meadows K, Armond AG (1997) Recurrence of primary pneumothorax. Thorax 52:805–809
15. Bense L, Eklund G, Odont D (1987) Smoking and the increased risk of contacting pneumothorax. Chest 92:1009–1012
16. Withers JN, Fishiback ME, Kiehl PV, Hannon JL (1964) Spontaneous pneumothorax. Am J Surg 108:772–776
17. Pinto LM, Dheda K, Theron G et al (2013) Development of a simple reliable radiographic scoring system to aid the diagnosis of pulmonary tuberculosis. PLoS ONE 8:e54235
18. Lee CY, Diloreto PC, Beaudoin J (1974) Catamenial pneumothorax. Obstet Gynecol 44:407–411
19. Laws HL, Fox LS, Younger B (1977) Bilateral catamenial pneumothorax. Arch Surg 112:627–628
20. Wilhelm JL, Scommegna A (1977) Catamenial pneumothorax: bilateral occurrence while on suppressive therapy. Obstet Gynecol 50:227–231
21. Tripp HF, Obney JA (1999) Consideration of anatomic defects in the etiology of catamenial pneumothorax. J Thorac Cardiovasc Surg 117:632–633
22. Chatman DL, Ward AB (1982) Endometriosis in adolescents. J Reprod Med 27:156–160

INTERNAL MEDICINE

□ CASE REPORT □

Cystic, Nodular and Cavitary Metastases to the Lungs in a Patient with Endometrial Stromal Sarcoma of the Uterus

Akiko Murakami[1], Takuo Hayashi[2,3], Yasuhisa Terao[4], Takanori Mori[1], Toshio Kumasaka[3,5], Kuniaki Seyama[1,3] and Kazuhisa Takahashi[1]

Abstract

A 57-year-old woman, who had undergone hysterectomy for uterine myoma 11 years earlier presented with cystic, nodular and cavitary lesions simultaneously visible on computed tomography images of the chest. Histological examinations of both the resected lung and past "myoma" specimens demonstrated that the original uterine tumor was a low-grade endometrial stromal sarcoma (ESS) that had metastasized to the lungs. No previous reports have described the coexistence of cystic, nodular and cavitary lesions with pulmonary metastasis of ESS; however, we successfully correlated the radiologic appearance with the corresponding pathologic findings. Medroxyprogesterone acetate therapy has effectively kept the patient asymptomatic for approximately five years.

Key words: pulmonary metastases, endometrial stromal sarcoma, pneumothorax, progesterone

(Intern Med 53: 1001-1005, 2014)
(DOI: 10.2169/internalmedicine.53.1946)

Introduction

Low-grade endometrial stromal sarcoma (ESS), a rare neoplasm comprising 0.2% of all uterine cancers and 15% of all uterine sarcomas (1), is classified separately from undifferentiated endometrial sarcoma. Low-grade ESS is histologically similar to proliferating endometrial stromal tissue, exhibits little cytological atypia or pleomorphism and is low in mitotic activity. The prognosis of patients with low-grade ESS is favorable in general, with a 10-year disease-free survival rates of 93% (2). However, approximately 40% of patients with low-grade ESS develop recurrent disease after long tumor-free intervals due to the slow-growing nature of the tumor (3). The major location of distant metastases is the lungs, with an incidence of pulmonary metastasis of 7% to 28% (4).

Pulmonary metastasis of low-grade ESS can manifest as various patterns on computed tomography (CT) images of the chest, including the presence of a solitary nodule, multiple nodules, multiple cysts and reticulonodular infiltrates (4-8). In patients with nodular pulmonary metastases of low-grade ESS, the differential diagnosis includes benign metastasizing leiomyoma (BML), carcinoid tumors, sclerosing hemangioma and metastasis of other neoplasms. On the other hand, cystic metastasis of low-grade ESS in the lungs should be carefully discriminated from lymphangioleiomyomatosis (LAM), mesenchymal cystic hamartoma and metastasis of leiomyosarcoma. However, the simultaneous coexistence of all of these imaging features in a single patient would result in a diagnostic dilemma.

In just such an experience, we encountered a patient with pulmonary metastasis of low-grade ESS who presented with cystic, nodular and cavitary lesions simultaneously. The patient had undergone hysterectomy and bilateral salpingo-oophorectomy due to uterine leiomyoma 11 years earlier. Pathologic and immunohistochemical examinations of her lung specimens greatly contributed to the ability to obtain a proper diagnosis, a rare pattern of pulmonary metastases of low-grade ESS, and provided a plausible explanation for the

[1]Division of Respiratory Medicine, Juntendo University Faculty of Medicine and Graduate School of Medicine, Japan, [2]Division of Human Pathology, Juntendo University Faculty of Medicine and Graduate School of Medicine, Japan, [3]The Study Group of Pneumothorax and Cystic Lung Diseases, Japan, [4]Division of Gynecology and Obstetrics, Juntendo University Faculty of Medicine and Graduate School of Medicine, Japan and [5]Department of Pathology, Japanese Red Cross Medical Center, Japan
Received for publication October 24, 2013; Accepted for publication November 28, 2013
Correspondence to Dr. Akiko Murakami, amuraka@juntendo.ac.jp

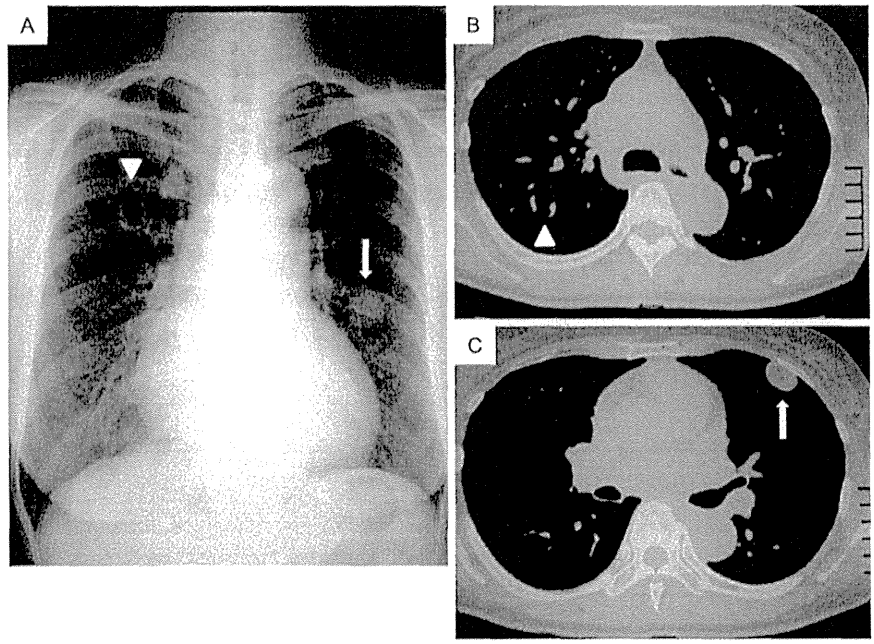

Figure 1. Radiologic findings in a patient with pulmonary metastasis of low-grade ESS. A: A chest radiograph obtained in September 2008 showed a cavitary nodule in the right upper lung field (arrowhead) and a solid nodule in the left middle lung field (arrow). B, C: Chest CT scans showing a cavitary nodule (18×15 mm) with an inhomogeneous wall thickness in the S^2 area of the right lung (corresponding to the shadow indicated by the arrowhead in A) and a solid nodule (20×12 mm) in the S^4 area of the left lung (corresponding to the shadow indicated by the arrow in A). Note the multiple thin-walled cysts scattered in the bilateral lung fields that are not visible on the chest radiograph.

mechanism of each imaging feature.

Case Report

A 57-year-old woman was referred to our hospital in September 2008 for a workup of right pneumothorax. A CT scan of the chest revealed several nodules, cavitary lesions and multiple thin-walled cysts. The patient's medical history disclosed that she was a farmer, had never smoked and had undergone hysterectomy and bilateral salpingo-oophorectomy for uterine myoma 11 years earlier. A physical examination was unremarkable. A laboratory examination showed a normal blood cell count with no biochemical abnormalities. Chest radiography demonstrated a cavitary nodule in the right upper lung field and a solid nodule in the left middle lung field (Fig. 1A). CT imaging of the chest supplemented these results by visualizing a cavitary nodule with an inhomogeneous wall thickness in the S^2 area of the right lung and a solid nodule in the S^4 area of the left lung, corresponding to the findings on the plain chest radiograph. Furthermore, several other solid and cavitary nodules (not shown) and multiple thin-walled cysts scattering throughout the bilateral lung fields were evident (Fig. 1B, C), although they had not been apparent on the chest radiograph. Under suspicion of a diagnosis of metastatic malignancy to the lungs, an enhanced CT scan of the abdomen and a whole-body combined ^{18}F-FDG positron emission tomography (PET)/CT scan were performed. However, both imaging studies failed to identify a possible extrapulmonary primary lesion. Instead, the ^{18}F-FDG PET/CT scan revealed mild ^{18}F-FDG uptake in several nodules and cavitary lesions in the right lung; the maximum standard uptake value (SUV_{max}) was within the range of 1.8 to 2.5. Unfortunately, the patient's left lung could not be evaluated on the ^{18}F-FDG PET/CT scan since she happened to have a mild degree of pneumothorax at the time of the PET examination. Thereafter, the left pneumothorax resolved spontaneously.

In December, the patient again developed left pneumothorax. Because her left lung was moderately collapsed, she was admitted to our hospital with a diagnosis of suspected BML of the uteri or the coexistence of an early stage of LAM and BML. Shortly after admission, right pneumothorax also developed and resolved immediately following the insertion of an intercostal chest tube. Meanwhile, the solid nodule in the S^4 area of the left lung exhibited cavitary formation (not shown). In contrast to the right pneumothorax, the left lung remained in a collapsed state with a continuous air leak from the chest tube. Accordingly, video-assisted thoracoscopic surgery (VATS) was performed for treatment as well as further diagnosis. Consequently, partial resection of the lingular lobe was performed, including the cavitary nodule in the S^4 area, with reinforcement of the resection line

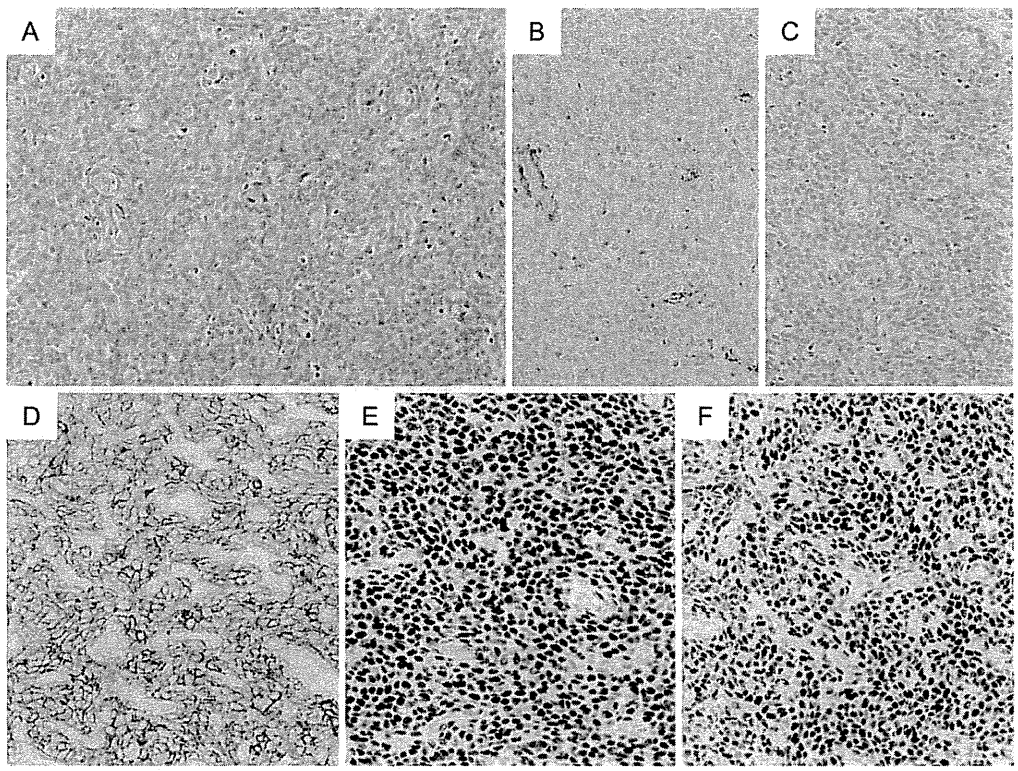

Figure 2. Histopathologic and immunohistochemical findings of the lingular lobe partially resected via video-assisted thoracoscopic surgery (VATS). The nodule (Fig. 1A, C), which had developed cavitary formation immediately prior to resection via VATS (Fig. 3A), was composed of dense, uniform proliferating tumor cells with oval-shaped nuclei (A: Hematoxylin and Eosin staining, high-power field). An immunohistochemical examination demonstrated that these cells were negative for α-smooth muscle actin (B: high-power field) and HMB45 (C: high-power field) and strongly positive for CD10 (D: high-power field). Meanwhile, the nuclei were strongly positive for estrogen receptor (E) and progesterone receptor (F).

using bioabsorbable non-woven fabric and partial ablation of the parietal pleura.

The pathologic examination of the resected lung specimen revealed dense and uniform proliferation of tumor cells with oval-shaped nuclei (Fig. 2A) in both the nodular portion and cavity wall of the left S^4 cavitary nodule (Fig. 3A). There was little cytological atypia or pleomorphism, and mitosis was scanty. However, tumor cells appeared in a whorl-like arrangement around the vessels. An immunohistochemical examination demonstrated the tumors cells to be negative for α-smooth muscle actin (SMA) (Fig. 2B) and HMB45 (Fig. 2C) and strongly positive for CD10 (Fig. 2D). The cell nuclei were strongly positive for estrogen receptor (ER) (Fig. 2E) and progesterone receptor (PR) (Fig. 2F). Since the immunohistochemical findings of the lungs indicated low-grade uterine ESS, we reviewed the hysterectomized specimen that had been diagnosed as a uterine myoma at a local hospital 11 years earlier. That tumor also consisted of oval-shaped cells in a whorl-like arrangement around the vessels and exhibited expansive growth with a partly irregular border and venous invasion at the periphery. Immunoreactivity for ER, PR and CD10 was positive, while that for both SMA and HMB45 was negative (not shown). Therefore, we concluded that the uterine tumor resected 11 years previously was a low-grade ESS that had subsequently developed pulmonary metastasis.

The cystic lesions scattered in the specimen from the resected lingular lobe were composed of ESS cells and normal alveolar septal cells. It is notable that the ESS cells frequently occupied airways leading into cysts and only connecting portions of the cyst wall, whereas most of the cyst wall was composed of normal alveolar septal cells (Fig. 3B). On the other hand, numerous small nodules composed of ESS cells, which were not evident on CT images, lay in the parenchyma (Fig. 3C). In addition, ESS cells had infiltrated the visceral pleura in some places, which may have contributed to the development of pneumothorax (Fig. 3D).

After establishing this diagnosis, we initiated the treatment with medroxyprogesterone acetate (MPA) administered orally at a dose of 400 mg/day. The solid and cavitary nodules disappeared within three to six months according to CT images of the chest. Some small cysts disappeared, although most remained unchanged. As of this writing, the patient has continued the MPA regimen and remained asymptomatic for approximately five years since its initiation. No new metastatic lesions have been identified.

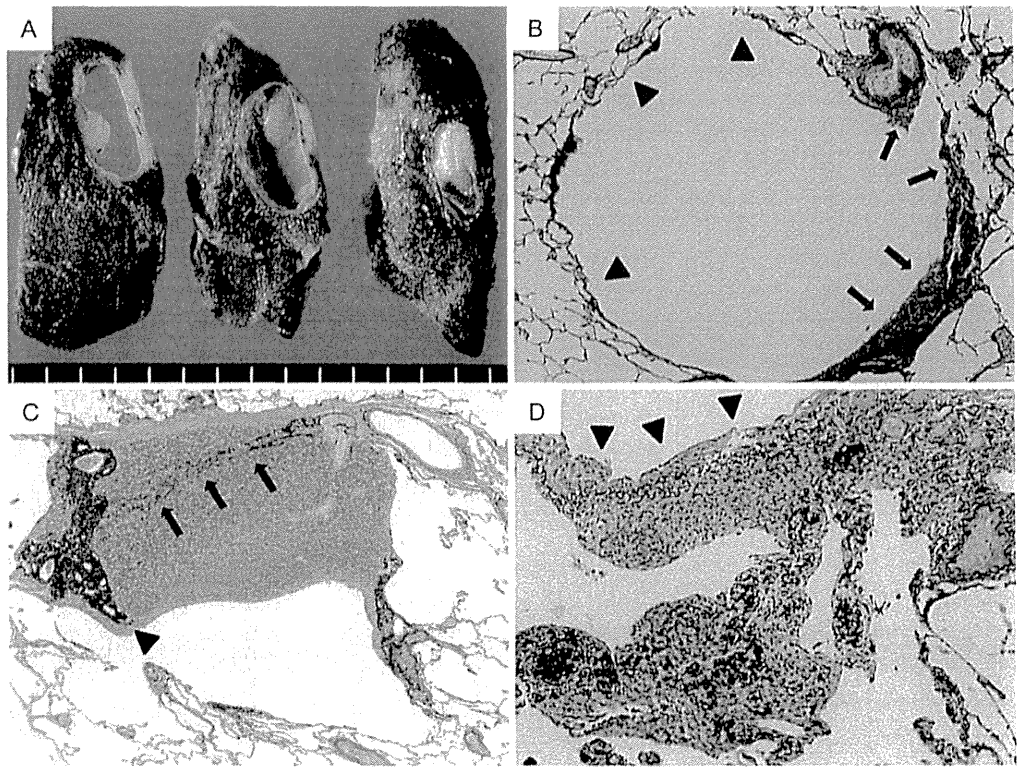

Figure 3. **Histopathologic lesions caused by proliferating ESS cells in the lungs. A: Macroscopic view of the resected lingular lobe specimen showing the cavitary nodule just beneath the visceral pleura. This nodule, which was present before VATS (Fig. 1A, C), partially underwent cavitary degeneration. The entire cavity wall was composed of ESS cells. B: Representative photomicrograph of a cystic lesion (approximately 5 mm in size). The cyst wall was primarily composed of normal alveolar septal cells (arrowhead). ESS cells were frequently present along airways connecting to the cysts (arrow), although they occupied only parts of the cyst wall (Elastica van Gieson staining, low-power field). C: Small areas of nodular proliferation of tumor cells were frequently visible in the lung parenchyma, although they were not clearly delineated on radiologic imaging (Elastica van Gieson staining, low-power field). Note that the elastic fibers formerly present in the alveolar walls were condensed towards the left side of the nodule (arrowhead) and eroded within the nodule (arrow). D: Representative photomicrograph of tumor cells infiltrating the visceral pleura. Elastic fibers in the pleura were disrupted by ESS cells (arrowhead) (Elastica van Gieson staining, mid-power field).**

Discussion

This report describes the case of a patient with low-grade ESS and pulmonary metastasis whose CT images of the chest showed cystic, nodular and cavitary lesions coexisting simultaneously. Although low-grade ESS of the uterus generally has a favorable prognosis, the tumor tends to develop pulmonary metastasis; metastasis occurs even if the primary tumor is resected and the patient experiences a long tumor-free interval. Aubery et al. reported intervals from hysterectomy to subsequent pulmonary metastasis ranging from 2.5 to 20 years (4). Since low-grade ESS is frequently present for long intervals before the appearance of pulmonary metastasis and CT scans show such varied patterns as the presence of a solitary nodule, multiple nodules, multiple cysts and reticulonodular infiltrates (4-8), selecting the correct diagnosis is often a challenge, especially when several radiologic manifestations coexist. In this context, our patient is a very rare example. Her simultaneous expression of cystic, nodular and cavitary lesions was not only unique, but also made the diagnosis problematic.

The mechanisms underlying the coexistence multiple lesions on radiologic examinations await final substantiation. However, based on the results of the histopathologic examinations in this case and the patient's clinical course, the following explanations have merit. First, the patient's cavitary lesions apparently evolved from the nodular proliferation of ESS cells, since a nodule in the S^4 area of the left lung demonstrated cavitary changes. Other researchers have asserted that the pathological mechanisms underlying the cavitary formation of a neoplasm include internal desquamation of tumor cells with subsequent liquefaction (9). Furthermore, we presume that the thin-walled cysts observed in this case developed due to the proliferation of ESS cells along peripheral small airways followed by the destruction of pa-